Surface studies of $A^{III}B^{V}$ compound semiconductors by ion channeling

A. Dygo and A. Turos
Soltan Institute for Nuclear Studies, Hoża 69, PL-00-681 Warsaw, Poland
(Received 18 November 1988; revised manuscript received 13 March 1989)

Backscattering-energy spectra were measured for 2-MeV He ions channeled in ⟨100⟩ GaP, GaAs, and InP single crystals with natural oxide surface layers. The analysis of the experimental spectra was performed by the Monte Carlo simulation. The simulation program is based on the binary-collision model. The influence of the surrounding atoms and the energy loss of the channeled particles were taken into account. Also, different types of the ion-atom potential were tested. The simulated channeling spectra were calculated with respect to the random yield which makes it possible to fit experimental spectra without any normalization. Based on the simulation program, the thickness of the surface oxide layer, thermal vibration amplitudes of crystal atoms, and random stopping power of incident ions were determined. The values obtained were compared with the previously published theoretical and experimental data.

I. INTRODUCTION

In the last decade ion channeling has become a well-established and valuable tool of surface science. The method was successfully applied to study the structure of clean surfaces as well as to characterize thin surface layers and interfaces.[1,2] Thermal surface-atom vibrations were also investigated with use of this method.[3] In all above applications accurate evaluation of a backscattering surface peak (SP) for an ideal bulklike surface is essential. This was usually performed by use of a standard Monte Carlo simulation technique.[4,5] However, the SP intensity obtained in this way is affected by inaccuracies of an ion-atom interaction potential and—most of all—by the used values of thermal vibrational amplitudes of atoms in crystals. Moreover, the necessity of the background subtraction leads to an uncertainty of the experimental SP evaluation. All these factors limit the sensitivity of the ion scattering-channeling technique as regards the determination of the structure of surfaces and interfaces.

In this paper we demonstrate that the above sources of errors can be substantially reduced by means of the Monte Carlo simulation of the whole backscattering-energy spectra instead of calculation of the SP intensity alone. The main idea underlying the method is to employ the experimental channeling spectrum itself for evaluation of needed physical quantities. In this manner, proper evaluation of the SP associated with an ideal surface can be made from the spectra obtained for real samples. By actually fitting the experimental spectrum in the region below the SP, the difference between measured SP and the SP for an ideal surface can be determined in the accurate way. This procedure, apart from enabling the reliable determination of the SP, simultaneously yields valuable information on the ion-atom interaction potential, vibrational amplitudes of bulk atoms, and ion stopping power in the investigated crystal. This comes into line with earlier studies on the yield oscillations in planar channeling[6,7] where potential and stopping-power information were obtained or recent attempts to study lattice dynamics and/or thermal vibrational amplitudes by ion channeling.[8,9] In contrast with those works which are based on the analysis of breakthrough or critical angles, our approach of direct fitting to the experimental spectrum offers better precision and is applicable to the axial as well as planar channeling.

The SP evaluation by the standard method becomes much more difficult in the case of binary-compound single crystals. The large errors associated with background subtraction in the region where the spectrum of the light component appears make this method quite unreliable. In contrast, our approach enables us to achieve improved accuracy for all components of a spectrum.

In this paper we report the results of channeling analysis of GaP, GaAs, and InP single crystals. No care was taken to avoid the formation of thin oxide surface layers. The applicability of the method for analysis of clean surfaces is obvious.

II. EXPERIMENTAL

The backscattering-channeling measurements were performed with 2-MeV He ions. The beam current was kept at 5 nA and the beam angular divergence was about 0.01°. Samples of ⟨100⟩ GaP, GaAs, and InP single crystals[10] covered by a natural oxide surface layer (after mechanical and chemical polishing) were mounted on a three-axis goniometer having an angular resolution of 0.025°. The scattering chamber was evacuated to a pressure of about 10^{-6} Torr. A liquid-nitrogen–temperature cold finger was placed in the vicinity of a sample. The carbon buildup on a sample surface was observed during the measurements, although the accumulated amount of it was small [$(1-5)\times10^{16}$ atoms/cm^2]. The analysis beam-induced damage to the sample was kept as low as possible by not exceeding a total beam fluence of 6×10^{15} ions/cm^2 (Ref. 1). The results presented were checked to be reproducible by repeating the measurements several times.

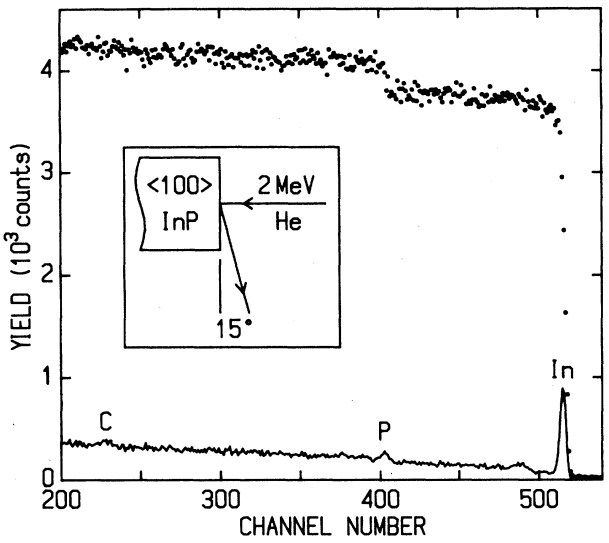

FIG. 1. Channeling (line) and random (dots) spectra for 2-MeV He ions scattered on ⟨100⟩ InP, measured with the grazing-exit-angle geometry.

In order to improve the depth resolution of the backscattering spectra, the grazing-exit-angle (15°) geometry was used with scattering angle of 105°. Typical spectra (aligned and random) for ⟨100⟩ InP are shown in Fig. 1. The exit angle of 15° was found to be the best for the observation of an oscillatory structure in the channeling spectrum below the SP. This structure—crucial for our analysis—becomes less pronounced when one changes to the "more grazing" angles, usually employed for maximizing the ratio of the SP to the background level. With the overall energy resolution of the detecting system ranging from 15 to 20 keV, the depth resolution was 100–130 Å. To measure the random spectrum—used for normalization–the sample was rotated by 360° (or multiples thereof) about an axis normal to the sample surface. The axis was tilted by several degrees with respect to the beam direction (critical angles for the investigated strings vary from 0.5° for P to 0.9° for In).

III. MONTE CARLO SIMULATION ANALYSIS

A. Simulation program

A detailed review of channeling simulation programs already described in the literature has been recently given by Smulders and Boerma.[11] Our approach of the modified binary collision model generally follows the well-known work of Barrett,[4] although essential extensions were added. First of all, in addition to the binary collisions of a projectile with the nearest crystal atom, the influence of surrounding atoms via binary collisions is also taken into account. Next, energy loss of the channeled particle is included in the calculation and the backscattering spectrum is determined directly rather than through the nuclear-encounter-probability–versus–depth relation. Also added is electronic multiple scattering.

In calculation of the deflection function $\vartheta(b)$, for an impact parameter b, a screened Coulomb potential is assumed,

$$V(r)=\frac{Z_1Z_2e^2}{r}u(r) . \tag{1}$$

To investigate the sensitivity of the simulation to the choice of the potential, three forms of the screening function $u(r)$ were considered.

(a) The independent-particle–model (IPM) atomic screening function[12]

$$u(r)=\{H[\exp(r/da_0)-1]+1\}^{-1} , \tag{2}$$

where $H=dZ_2^{0.4}$ and d is an adjustable parameter given in Ref. 12.

(b) The Ziegler-Biersack-Littmark (ZBL) "universal potential"[13]

$$u(r)=\sum_{i=1}^{4}c_i\exp(-b_ir/a) , \tag{3}$$

with

$$\{c_i\}=\{0.02817,0.2802,0.5099,0.1818\} ,$$

$$\{b_i\}=\{0.2106,0.4029,0.9423,3.2\} ,$$

and

$$a=0.8853a_0(Z_1^{0.23}+Z_2^{0.23})^{-1} .$$

(c) The classic Molière screening function[14]

$$u(r)=\sum_{i=1}^{3}c_i\exp(-b_ir/a) , \tag{4}$$

with

$$\{c_i\}=\{0.35,0.55,0.1\} ,$$

$$\{b_i\}=\{0.3,1.2,6.0\} ,$$

and the Firsov's screening length

$$a=0.8853a_0(Z_1^{1/2}+Z_2^{1/2})^{-2/3} .$$

The deflection function is calculated from the exact scattering integral by means of the Gauss-Mehler quadratures[15,16] and tabulated for use in the simulation code. Simple linear interpolation between tabulated values allows for both good accuracy (better than 0.2%) and time efficiency. The deflection functions for the investigated systems, calculated for the three potentials (relative to the Molière-potential values), are compared in Fig. 2. The differences between values obtained for various potentials are clearly visible.

Random thermal displacements of crystal atoms are chosen according to the Gaussian distribution. Only displacements perpendicular to the channel axis are considered. The choice of the root-mean-square amplitudes of the thermal vibrations is discussed in the next subsection. To economize on computing time, displacements with the Gaussian distribution are stored in an array (1000 elements) and selected randomly. The generalized feedback–shift-register method[17] is employed for random number generation.

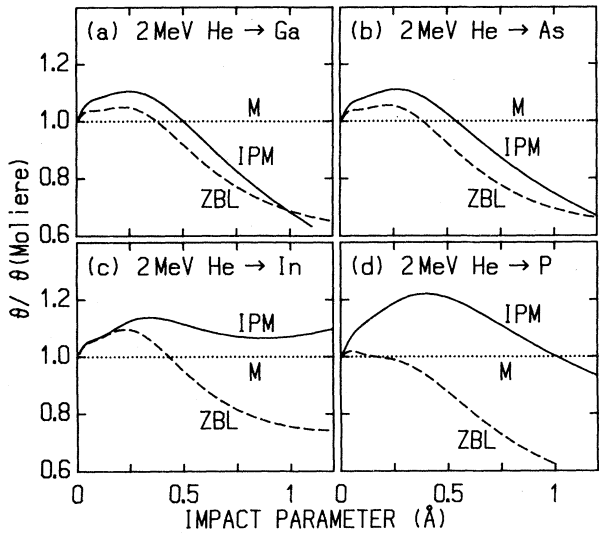

FIG. 2. Deflection functions for the IPM and ZBL potentials, presented relative to the Molière-potential values, for 2-MeV He scattering on (a) Ga, (b) As, (c) In, and (d) P.

Energy losses of channeled ions are evaluated within the three-component model.[18] Applying it to an AB compound crystal we assume Bragg's rule of additivity of the random stopping cross sections. Then the random stopping cross section in the compound, ϵ_r^{AB}, can be written

$$\epsilon_r^{AB}=\epsilon_r^A+\epsilon_r^B=\epsilon_c^A+\epsilon_{v1}^A+\epsilon_{v2}^A+\epsilon_c^B+\epsilon_{v1}^B+\epsilon_{v2}^B \ , \tag{5}$$

where superscripts A and B refer to the compound's atoms, ϵ_c is the stopping due to the core electrons, ϵ_{v1} is the stopping due to the single-particle excitations of the valence electrons, and ϵ_{v2} is the stopping due to plasmon excitations. The last two terms (for atom A) are given by

$$\epsilon_{v1}^A=\frac{4\pi Z_1^2e^4}{m_ev^2}Z_v^A\ln\left[\frac{2m_evv_F}{\hbar\omega_p}\right] \tag{6}$$

and

$$\epsilon_{v2}^A=\frac{4\pi Z_1^2e^4}{m_ev^2}Z_v^A\ln\left[\frac{v}{v_F}\right] \ , \tag{7}$$

where Z_1 is the atomic number of the incident ion, v its velocity, m_e is the electron mass, and Z_v^A is the number of valence electrons per A atom. In the above formulas, the Fermi velocity v_F and the plasmon energy $\hbar\omega_p$ are calculated for the average density of valence electrons in the AB crystal. Thus, replacing in Eqs. (6) and (7) Z_v^A by Z_v^B—the number of valence electrons per B atom—one obtains expressions for ϵ_{v1}^B and ϵ_{v2}^B, respectively. ϵ_c^A (ϵ_c^B) is calculated based on the random stopping ϵ_r^A (ϵ_r^B), $\epsilon_c^A=\epsilon_r^A-(\epsilon_{v1}^A+\epsilon_{v2}^A)$. The random stoppings ϵ_r^A and ϵ_r^B are taken according to Ziegler's formula.[19]

Local (channeling) stopping power is now written as

$$\epsilon^{AB}(r)=\frac{n_c^A(\mathbf{r})}{n_c^A}\epsilon_c^A+\frac{n_v^A(\mathbf{r})}{n_v^A}\epsilon_{v1}^A+\frac{n_c^B(\mathbf{r})}{n_c^B}\epsilon_c^B+\frac{n_v^B(\mathbf{r})}{n_v^B}\epsilon_{v1}^B+\epsilon_{v2}^{AB} \ , \tag{8}$$

where n_c^A and n_c^B are the average densities of core electrons, and n_v^A and n_v^B of valence electrons for respective atoms, while the quantities denoted as functions of position $\mathbf{r}$ are respective local densities. The last term, $\epsilon_{v2}^{AB}=\epsilon_{v2}^A+\epsilon_{v2}^B$, gives a position-independent contribution to the stopping. Hence, the energy lost by an ion in a single collision with, say, an atom A for an impact parameter b is given by

$$\Delta E^A(b)=\epsilon_c^AL_c^A(b)+\epsilon_{v1}^AL_v^A(b) \ , \tag{9}$$

where $L_c^A(b)$ and $L_v^A(b)$ are functions of electronic density for atom A, defined in Ref. 18. They are calculated using the Roothaan-Hartree-Fock atomic wave functions.[20]

Energy losses according to Eq. (9) are tabulated for various impact parameters (with step size of 0.001 Å) and employed by the simulation code. As the penetration depth considered in our simulation is small (usually less than 4000 Å), constant energy of ingoing particles is assumed when calculating channeling energy losses. Similarly, two constant energies of particles scattered at different crystal atoms A and B are used for determining random energy losses along the outgoing path. These are average values of energies of particles penetrating into the region of the peak below the SP, observed in channeling spectra (see Sec. III C).

The depth-to-energy relation for the grazing–exit-angle geometry is governed mainly by the random stopping for the outgoing path. Accordingly, one cannot expect the resulting spectra to be strongly influenced by the energy-loss model used for channeled ions. Additional calculations performed using the Lindhard model,[21,18] indeed yielded insignificant differences as compared to the three-component model (see Sec. III C).

The electronic multiple scattering according to Lindhard[21] is included as an option in the simulation program. Random deflections related to this scattering are chosen according to the Gaussian distribution with the one-dimensional standard deviation

$$\sigma=\left[\frac{1}{2}\frac{m_e}{M_1}\frac{\Delta E}{E}\right]^{1/2} \ , \tag{10}$$

where M_1 is the ion mass and ΔE is the energy lost in a single ion-atom collision [cf. Eq. (9)]. The effect of the electronic multiple scattering on simulated spectra was found to be small, as shown in Sec. III C.

One of the most important elements of our approach is the method of calculation of backscattering-energy spectra. Contrary to other simulations,[22] this is performed relative to the random yield. The comparison of a simulated spectrum with an experimental one (also normalized to the respective random yield) is thus made on an absolute basis rather than through an adjustable normalization constant. Besides, the calculation of the spectrum

relative to the random one allows us to neglect the energy dependence of the cross section. In this approximation the normalized nuclear encounter probability[4] for a particle moving with an impact parameter b with respect to the equilibrium lattice position of crystal atom is given by the ratio of the areal atomic density $P(b)$, sensed by the channeled particle, to the areal atomic density for the random incidence, i.e.,

$$Y(b)=\frac{P(b)}{1/A_0}=A_0\frac{1}{2\pi u_1^2}\exp\left[-\frac{b^2}{2u_1^2}\right]. \quad (11)$$

A_0 represents perpendicular area associated with one strong and u_1 is the one-dimensional root-mean-square thermal vibration amplitude. The above contribution is accumulated in the appropriate spectrum channel according to the current energy of the particle. Simultaneously, the resulting nuclear encounter probability as a function of a penetration depth is found.

Particles incident upon the crystal surface with large impact parameters, having small transverse energy, are unlikely, on their considered path, to come sufficiently close to an atom to produce any significant contribution [given by Eq. (11)] to the spectrum. Therefore, in the case of a beam incident parallel to an axial channel, only particles with sufficiently large transverse energy are followed. The maximum impact parameter for these particles is determined based on the continuum approximation. The amount of the particles followed in the calculation is about 10% of all particles which uniformly irradiate the crystal surface. This enables the reduction of the computing time by a factor of about 10.

Particles scattered through more than a given angle (typically 3°) are regarded as dechanneled. It is noteworthy that in the case of axial channeling the fraction of dechanneled particles (in the above sense) is extremely small. For example, out of 5.1×10^5 He ions of 2 MeV energy, incident on ⟨100⟩ GaP (in a calculation for the ZBL potential), only 43 (0.01%) become dechanneled within the first 25-Å-thick surface layer; additional 389 ions (0.08%) become dechanneled when the penetration depth is increased up to 3000 Å. Nevertheless, in addition to the yield contribution from channeled ions [given by Eq. (11)], the contribution from dechanneled ones is also taken into account in the program. As the majority of them are scattered at a small forward angle, each dechanneled ion is assumed to contribute like particles moving randomly.

There are also two preset maximum impact parameters used in the program. For impact parameters greater than the first limit (typically 1.5 Å), the changes in the direction of particle's motion are neglected, whereas for impact parameters greater than the second limit (typically 2 Å) the energy loss associated with close collisions with the atom's electrons [as given by Eq. (9)] is no longer taken into account. The above procedure applies both to the nearest atom and to surrounding ones.

The program assumes perfect crystal structure with abrupt termination at the surface. Possible surface layers affect particles' trajectories primarily through the (nuclear) multiple scattering.[23] It can be well approximated by introducing adequate angular divergence of the incident beam, provided characteristics of the surface layers are known prior to analysis. If this is not the case, one can treat the beam divergence as a fitting parameter. Here we assume a Gaussian angular distribution of incident directions, its standard deviation being an adjustable parameter. This is based on the fact that scattering by thick layers—where the effect is strongest—produces asymptotically a Gaussian distribution. In the case of thin layers (approximately below 10^{17} atoms/cm^2) respective distribution deviates noticeably from a Gaussian, falling off more slowly. However, the magnitude of the effect in this case is correspondingly smaller, and so is its influence on simulated spectra. In fact, as is shown in Sec. III C, this influence in the case of our measurements is negligible.

Additional beam divergence results from the finite sizes of beam collimators used in experiments. In our approach it increases, accordingly, the standard deviation of the assumed Gaussian distribution. In the following, this standard deviation is cited as a measure of the beam divergence used in calculations.

B. Thermal vibration amplitudes

The choice of the thermal vibration amplitudes of crystal atoms is of fundamental importance for the shape of the calculated spectrum and, in particular, for the SP intensity obtained. Often the Debye theory is applied with the Debye temperature θ_D taken from a handbook. However, it has long been realized that there are various θ_D's, depending on the method by which they were determined.[24] Debye-temperature values given in standard handbooks are usually determined by the calorimetric methods and are known to yield overly low thermal vibration amplitude. More realistic are the so-called x-ray Debye temperatures θ_M, determined by the x-ray diffraction or neutron scattering methods.[24–27] In the case of $A^{III}B^{V}$ compound semiconductor crystals reliable and consistent data on θ_M or the vibration amplitudes are still missing.[28] This is illustrated in Table I, where root-mean-square vibration amplitudes for the investigated crystals, extracted from the published data, are reported. One notes wide scattering of the values listed, persisting up to the recent measurements.[29] As simulated channeling spectra are very sensitive to the magnitude of thermal vibration amplitudes, the possibility of independent determination of these amplitudes is made feasible by fitting experimental spectra with simulated spectra. This procedure turned out to be quite successful, as is shown in the next subsection.

The problem of equal-time displacement correlations and their influence on channeling simulations was investigated by Jackson and Barrett.[30] They have shown that displacement correlations may cause a decrease of the SP intensity and the minimum yield of about 10%. The equivalent decrease of the SP and the minimum yield can be simulated by a similar change of uncorrelated vibration amplitudes. Thus, determining the amplitudes by simulation which assumes no correlation, one finds their effective value which incorporates the effects of correlations.

TABLE I. One-dimensional root-mean-square amplitudes of thermal vibrations at room temperature for GaP, GaAs, and InP, extracted from the published data. A and B refer to the type of atom in the compound $A^{III}B^{V}$.

	u_1^A (Å)	u_1^B (Å)	$\bar{u}_1$ (Å)	Method[a]
GaP			0.081	RIM[b]
	0.068	0.070		RIM[c]
	0.086	0.100		XD[d]
	0.078	0.095		XD[e]
	0.079	0.088		XD[e]
	0.080	0.087		XD[f]
	0.081	0.090		SM[g]
GaAs			0.100	ND[h]
			0.100	RIM[b]
			0.048	LEED[i]
			0.107	XD[j]
			0.065	LEED[k]
	0.073	0.073		RIM[c]
			0.084	LEED[l]
	0.072	0.072		RIM[m]
	0.089	0.082		XD[d]
			0.087	XD[n]
			0.089	XD[n]
	0.098	0.092		XD[e]
			0.094	XD[e]
	0.091	0.094		SM[g]
	0.093	0.073		XD[o]
InP	0.080	0.082		RIM[c]
	0.080	0.080		RIM[m]
	0.100	0.116		XD[d]
	0.107	0.086		VSM[g]

[a]Theory—rigid-ion model (RIM), shell model (SM), valence-shell model (VSM); experiment—x-ray diffraction (XD) neutron diffraction (ND), low-energy electron diffraction (LEED).
[b]R. Banerjee and Y. P. Varshni, Can. J. Phys. **47**, 451 (1969).
[c]J. F. Vetelino, S. P. Gaur, and S. S. Mitra, Phys. Rev. B **5**, 2360 (1972).
[d]V. T. Bublik and S. S. Gorelik, Krist. Tech. **12**, 859 (1977).
[e]R. N. Kyutt, Fiz. Tverd. Tela (Leningrad) **20**, 395 (1978) [Sov. Phys.—Solid State **20**, 227 (1978)].
[f]H.-G. Bruhl, Krist. Tech. **15**, K83 (1980).
[g]Reference 28.
[h]G. Arnold and N. Nereson, Phys. Rev. **131**, 2098 (1963).
[i]A. Yu. Mityagin, V. P. Orlov, and V. M. Brylov, Fiz. Tverd. Tela (Leningrad) **12**, 2321 (1970) [Sov. Phys.—Solid State **12**, 1854 (1970)].
[j]R. Uno, T. Okano, and Y. Yukino, J. Phys. Soc. Jpn. **28**, 437 (1970).
[k]B. A. Nesterenko, A. D. Borodkin, and O. V. Snitko, Surf. Sci. **32**, 576 (1972).
[l]B. A. Nesterenko, A. D. Borodkin, and O. V. Snitko, Fiz. Tverd. Tela (Leningrad) **15**, 2602 (1973) [Sov. Phys.—Solid State **15**, 1731 (1973)].
[m]D. N. Talwar and B. K. Agarwal, J. Phys. C **7**, 2981 (1974).
[n]T. Matsushita and J. Hayashi, Phys. Status Solidi A **41**, 139 (1977).
[o]Reference 29.

C. Fitting to experimental spectra

The program described above was applied to simulate backscattering spectra for 2-MeV He ions channeled in ⟨100⟩ GaP, GaAs, and InP single crystals. When comparing the results with the experimental spectra one should take into account the oxide and carbon surface layers present in the investigated crystals (cf. Sec. II). The effect of these layers on the spectra measured is essentially threefold: (a) C and O peaks appear, superimposed on the substrate background, (b) the SP's due to the crystal atoms increase, and (c) the beam angular divergence is increased through the multiple-scattering effect.

C and O peaks do not interfere with the comparison between experimental and simulated spectra because their energies are sufficiently low. As mentioned in Sec. II, the amount of carbon atoms was estimated to be $(1-5)\times10^{16}$ atoms/cm^2, depending on the measurement. Very poor statistics of the oxygen peaks in all measurements renders determination of the amount of oxygen atoms impossible. At any rate it is much less than the amount of carbon atoms.

The analysis of the SP's due to the crystal atoms is given in the next section. Based on the results of Stensgaard *et al.*[5] and on average thermal vibration amplitudes deduced from Table I, it can be estimated from the experimental spectra that the amount of substrate atoms in the oxide layer is of the order of 2.5×10^{15} atoms/cm^2 (1 atom/row).

In order to estimate the influence of these surface layers on the beam divergence, angular distributions according to the multiple-scattering theory of Sigmund and Winterbon[23] were calculated. Figure 3 presents the nor-

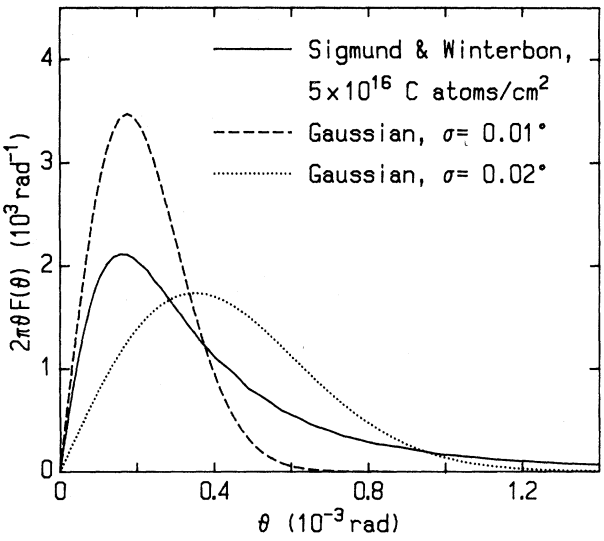

FIG. 3. Normalized (radial) angular distribution for 2-MeV He-ion beam multiply scattered in a layer of 5×10^{16} carbon atoms/cm^2, calculated according to Ref. 23 (solid line), in comparison with Gaussian distributions with the standard deviations of 0.01° (dashed line) and 0.02° (dotted line).

malized radial distribution, $2\pi\theta F(\theta)$, calculated for the thickness layer of 5×10^{16} C atoms/cm^2, in comparison with two Gaussian distributions having standard deviations of 0.01° and 0.02°. One notes that the maximum of the obtained distribution agrees with the maximum of the Gaussian with a standard deviation of 0.01°, while most of its large-angle tail is contained in the Gaussian with a standard deviation of 0.02°. The effect of the other surface atoms is significantly smaller. One can only speculate about details of an angular distribution of the primary beam obtained from an accelerator. In any event, its standard deviation does not exceed 0.01° and—contrary to the angular distributions due to multiple scattering—it most likely has a sharp cutoff at a maximum angle. Thus, the assumption of a Gaussian distribution with a standard deviation of 0.01° or 0.02° that represents an overall angular divergence of the beam seems to be reasonable. At least it should enable us to perceive the effect of an angular divergence on simulated spectra if there is any.

As mentioned in Sec. III A, the comparison between simulation and measurements is made for spectra normalized to the respective random yields. This procedure eliminates efficiency-calibration errors and, putting the comparison on an absolute basis, i.e., without any arbitrary parameters, enables reliable determination of the thermal vibration amplitudes. On the other hand, it allows us to neglect the energy dependence of the scattering cross section, since this dependence is to a good approximation canceled out by dividing the channeling spectrum by the random one. Normalization to the random yield of the heavier element of the compound is consistently used in this paper. When normalizing an experimental spectrum, the linear dependence of the random yield on energy was assumed, which is sufficiently good approximation in the energy interval of interest. In the case of GaAs, for which the spectrum components due to the individual elements of the compound cannot be resolved, a perfect stoichiometry was assumed in order to determine the As contribution.

Before presenting the final results of the simulation let us first demonstrate the effect of the change of different simulation parameters. Figure 4 shows a number of the simulated spectra (curves $A-E$) together with the experimental one (histogram) for the GaP single crystal. The IPM ion-atom potential and Ziegler's random stopping power were used in the calculations. Spectra A and B correspond to the vibration amplitudes $u_1^{Ga}=u_1^{P}=0.068$ Å deduced from the Debye temperature $\theta_D=445$ K (Ref. 31). According to the discussion in the preceding subsection, the calculated yield appears too low in comparison with the experimental one. Spectrum A was calculated for a perfectly collimated beam, while spectrum B corresponds to an intentionally large beam divergence of 0.1°. Hence the observed difference between experimental and calculated yields cannot be attributed to the presence of oxide and carbon surface layers, as their influence on the beam divergence was estimated to be much lower. Spectra C, D, and E correspond to the increased vibration amplitudes $u_1^{Ga}=0.084$ Å and $u_1^{P}=0.086$ Å. They match the experimental yield quite

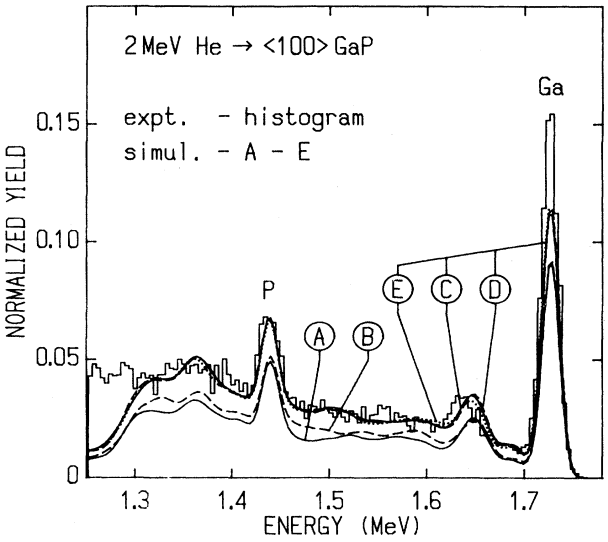

FIG. 4. Experimental (histogram) and simulated (curves $A-E$) backscattering spectra for 2-MeV He ions channeled in ⟨100⟩ GaP (see text).

well although a difference persists in the position of the peak below the SP for Ga. This can be attributed to the energy-loss model used in the calculations. The three-component model of channeled particle energy loss was applied for calculation of the spectrum C while spectrum D was calculated using the Lindhard model. It seems that choice of the energy-loss model has only limited influence on the simulated spectra, as can be expected for the grazing–exit-angle geometry. The influence of the electronic multiple scattering, which is included in spectrum E, also appears to be small. All three spectra C, D, and E indicate that in order to match the experimental peak at 1.63 MeV an increase of the random stopping power is needed.

According to the above discussion, when fitting simulated spectra to the experimental ones, thermal vibration amplitudes and random stopping power were varied. The final calculations were performed for the three-component model of channeled ion energy loss, including the electronic multiple scattering, and for the beam divergence of 0.01°. It should be pointed out that changing the beam divergence to 0.02° virtually has no influence on the resulting spectra. If higher values of the divergence are used, it affects the spectra mainly below the first subsurface peak (cf. curves A and B in Fig. 4). As a consequence, the yield in the simulated spectrum increases faster with decreasing energy than in the experiment, which makes it impossible to reproduce the experimental spectra by adjusting the vibration amplitudes. This observation is consistent with the estimates of the thickness of the surface layers (and their influence on the beam divergence) given at the beginning of this subsection, as well as with the final results on the thickness of the surface-oxide layers, presented in Sec. III D.

To investigate the influence of the ion-atom potential, the fitting was repeated for the IPM, ZBL, and Molière

potentials. In order to assess statistical deviations, four (statistically) independent runs were performed for each potential, without changing the final parameters. Usually $(1-1.5)\times10^4$ particle trajectories were calculated in a single run (applying nonuniform irradiation, cf. Sec. III A), which yielded total effective statistics for four runs of $(3-6)\times10^5$ particles. The spectra presented below are averages of individual runs. Statistical errors are very small (at most few curve thicknesses) and were not indicated in the figures.

The final results of simulation for GaP together with the experimental spectrum are shown in Fig. 5. As can be seen, excellent fits to the experimental data were obtained—except for the SP's—for all investigated potentials. A small rise of the experimental yield with respect to the simulated spectra is observed below the phosphorous SP. Its position corresponds exactly to a surface peak for silicon (indicated by an arrow in Fig. 5). A surface impurity of silicon was suspected in the crystal on the grounds of the employed procedure of the surface preparation. Based on the comparison between the experimental and simulated spectra, it can be concluded that the amount of silicon present at the crystal surface is much smaller than the thickness of the carbon layer (the main factor affecting the beam divergence), and its influence on the simulation results is negligible.

The amplitudes of thermal vibration and the random stopping power used in the simulations are given in Table II. In the course of seeking the best value of these quantities, a number of adjacent values have been tried. Since the statistical deviations in the simulated spectra were very small (as discussed above), it allowed us to estimate fitting errors quite accurately. The errors given in Table II set limits on the range of acceptable values. If a given quantity is changed beyond its error limits, it will result in a noticeable deterioration of the corresponding fit to the experimental spectrum.

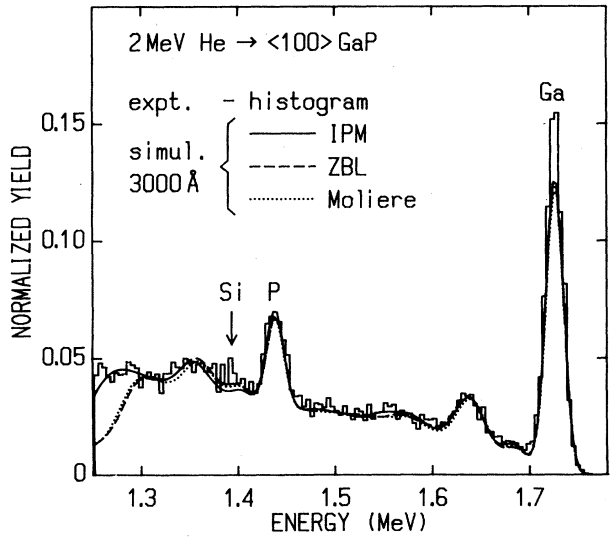

FIG. 5. Experimental and simulated backscattering spectra for 2-MeV He ions channeled in ⟨100⟩ GaP. Simulated spectra correspond to the IPM, ZBL, and Molière potentials; penetration depth is 3000 Å.

TABLE II. Thermal vibration amplitudes and random stopping powers used in the simulations for GaP, GaAs, and InP (The numbers in parentheses are estimated fitting errors on the last digit shown.) A and B refer to the type of atom in the compound $A^{III}B^{V}$.

	Potential	u_1^A (Å)	u_1^B (Å)	Random stopping[a]
GaP	IPM	0.084(1)	0.086(2)	1.10(1)
	ZBL	0.088(1)	0.083(2)	1.02(1)
	Molière	0.084(1)	0.086(2)	1.02(1)
GaAs	IPM	0.100(2)	0.105(2)	1.05(2)
	ZBL	0.100(2)	0.105(2)	1.00(2)
	Molière	0.102(2)	0.102(2)	1.00(2)
InP	IPM	0.116(1)	0.118(2)	1.03(1)
	ZBL	0.116(1)	0.118(2)	1.00(1)
	Molière	0.114(1)	0.116(2)	0.97(1)

[a]Relative to Ziegler's data (Ref. 19) (assuming Bragg's rule).

It should be noted that the best values of the vibration amplitudes and the random stopping power are potential dependent. The differences are of about a few percent only, but nevertheless they are beyond the estimated errors. Thus, one cannot discriminate between the potentials studied, based solely on the analyzed spectrum. However, if more precise data on the random stopping power were available, it would be possible to determine the best potential and the more accurate vibration amplitudes. The vibration amplitudes for GaP, determined for the IPM and Molière potentials (cf. Table II), are in a good agreement with some experimental results listed in Table I and with the most reliable theoretical estimate of Reid.[28] In the case of the ZBL potential, the vibration amplitude for Ga (0.088 Å) is greater than that for P (0.083 Å), contrary to all other results. As mentioned in the previous subsection, vibration correlations are expected to decrease vibration amplitudes obtained by our method. Thus, in view of a general agreement found between our amplitudes and those from different sources, the influence of correlations does not appear to be significant.

The comparison between the spectra simulated for different potentials and the experimental one for GaAs is presented in Fig. 6. The simulated spectra agree well with the experiment although the fit is not as good as in the case of GaP. This can be attributed to the difficulties in fitting a spectrum composed of two completely overlapping components. The thermal vibration amplitudes and the random stopping powers obtained for various potentials (cf. Table II) are—as in the previous case—slightly different. The vibration amplitudes obtained for GaAs are in reasonable agreement with the average values listed in Table I, although they are somewhat larger. The amplitude for As atoms, used for the IPM

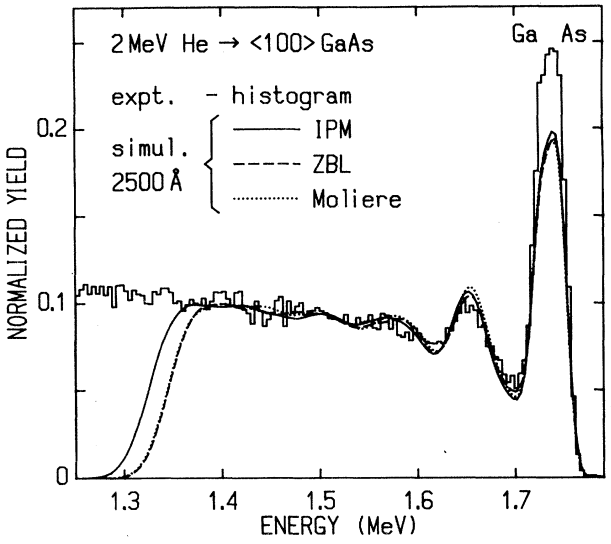

FIG. 6. Same as in Fig. 5 for GaAs; penetration depth is 2500 Å.

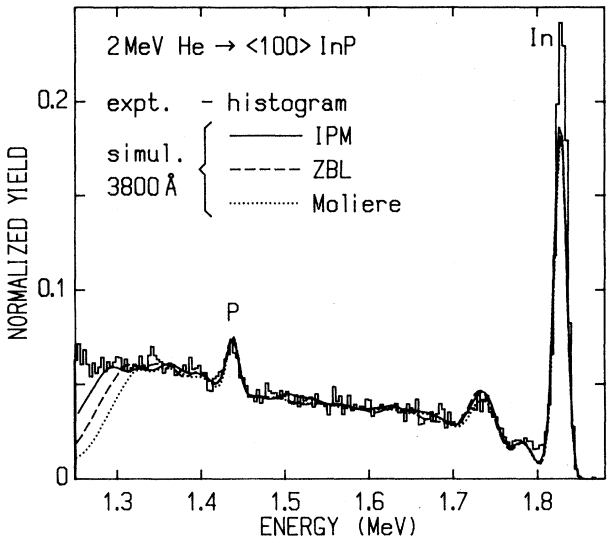

FIG. 7. Same as in Fig. 5 for InP; penetration depth is 3800 Å.

and ZBL potentials (0.105 Å), is greater than that for Ga atoms (0.1 Å). This is contrary to all x-ray results, but in agreement with the shell-model predictions.[28]

Figure 7 presents the best fit of the simulated spectra for InP in comparison with the experimental one. As can be seen, the agreement is nearly as good as in the case of GaP, although the statistics of the experimental spectrum is poorer. This is particularly clear for the experimental phosphorus SP, which is seen to be smaller than the simulated ones. The data on the vibration amplitudes for InP are especially scarce and inconsistent (cf. Table I). As listed in Table II, the amplitudes used in the simulations are in general larger than the previously published ones.

At this point we would like to comment on the possible presence of imperfections in the investigated single crystals and on their influence on the results of our analysis. The present simulations demonstrate that the characteristic oscillatory shape of the backscattering spectra for the systems studied is in a direct way connected with the (perfect) crystallographic structure assumed in the calculations. This shape exhibits yield oscillations with the pronounced subsurface peak, superimposed on a background which rises slowly with decreasing energy. When the amplitude of thermal vibrations is changed in the calculation (within reasonable limits), the average yield in the resulting spectrum changes accordingly, but the spectrum shape is basically retained. Thus, the almost perfect matching of an experimental spectrum with the shape of the calculated one gives evidence of very good crystal quality. At the same time it proves that the inferred thermal vibration amplitudes are not overestimated. If an appreciable amount of imperfections were present in the crystals, it would result not only in an increase of the average backscattering yield, but also in a smoothing over of the oscillatory structure of the spectrum. Such an effect was indeed observed during prolonged irradiation of the crystals. That is why as a low beam fluence as possible was used in the measurements (see Sec. II).

D. Surface-peak analysis

In applying our simulation program to analyze the SP intensity for the investigated samples, we make the usual assumption that the observed intensity comes from the crystalline substrate and nonregistered crystal atoms present in the surface-oxide layer.[1,32] The substrate contribution can be accurately determined by the simulation program which assumes an ideal bulklike surface structure. Then the difference between the measured and calculated SP's gives direct information on the number of nonregistered crystal atoms in the surface oxide. Certainly, based on our single measurement, nothing can be said about possible structure of this layer.

As mentioned in Sec. III A, the simulation program is used not only to calculate an energy spectrum, but it simultaneously yields the nuclear encounter probability (NEP) as a function of depth. The latter quantity is best suited for the SP intensity determination. Figure 8 presents the comparison between the simulated energy spectrum (dashed line) and the NEP (histogram) for the GaP case. The depth-to-energy relation associated with the random beam incidence was used to convert the NEP to a function of energy. The channel width corresponds to a depth interval of 25 Å. As can be seen, in this case over 90% of the SP intensity comes from the first 25-Å-thick surface layer.

The SP intensities associated with the ideal bulklike surface were determined based on the NEP obtained for each component of the investigated crystals. The results are summarized in Table III, where they are referred to as the calculated values.

The evaluation of the SP's for the experimental spectra is based on the total number of counts present in the region of a given SP, corrected for background counts. Ba-

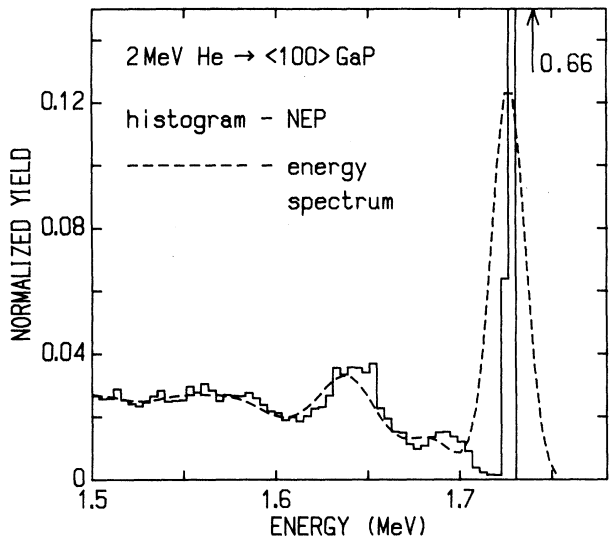

FIG. 8. Backscattering spectrum (dashed line) and related nuclear encounter probability (histogram) for 2-MeV He ions channeled in ⟨100⟩ GaP.

sically, there are two kinds of background in the case of binary compounds (cf. Figs. 5 and 7). One of them, related to the finite detecting-system resolution, is present in the SP for each component of the compound. The other one, pertaining to the lighter component only, comes from the portion of the spectrum due to the heavier component. Since simulated spectra reproduce experimental spectra very well, the former background correction was found as a difference between the total number of counts in the SP region in the simulated spectrum and the SP intensity derived from the related NEP (see Fig. 8). This difference was determined for each potential and then averaged in order to increase the statistics. The latter background correction was also evaluated based on the simulation results. It was taken as an average of the total yield (in the proper region) for the partial spectra corresponding to the heavier component, simulated for the three potentials. The final SP intensities determined for the experimental spectra are reported in Table III as the measured values. They are potential dependent, which is related exclusively to different stopping powers used for various potentials, as described in the preceding subsection. Differences between the measured and the calculated SP intensities are also given in Table III.

In the case of GaAs it was impossible to determine individual components for Ga and As (cf. Fig. 6). Therefore, in order to evaluate difference between the measured and the calculated SP's, the yield for the simulated spectra, integrated in the region encompassing both SP's, was subtracted from that for the experimental spectrum. Under the assumption of perfect stoichiometry, the difference in the SP's was the same for Ga and As.

Errors given in Table III for the measured values are the statistical ones. Deviations between the values corresponding to various potentials reflect an uncertainty due to the inaccuracy of the potential (stopping power). Errors for the calculated values were evaluated based on the four statistically independent runs performed for each case (cf. Sec. III C). Both kinds of errors were taken into account when determining errors in the difference between measured and calculated values.

It can be noted that the calculated SP intensities obtained for various potentials are quite consistent, although in some cases deviations greater than the estimated errors are observed. The same conclusion holds for the difference in the SP intensities. In the case of P in InP, this difference was negative, which can be attributed to rather poor statistics in the P peak in the experimental spectrum. The relative error was about 12%. Generally, it was found that the surface-oxide layer on the analyzed samples did not exceed approximately 1 atom/row. This layer appears to be smallest for GaP (about 0.7 atom/row), for which the best agreement between the simulated and experimental spectra was obtained (cf. Figs. 5–7).

IV. CONCLUSIONS

A method has been developed which makes it possible to reproduce accurately experimental backscattering spectra of channeled ions by means of the Monte Carlo

TABLE III. Surface-peak intensity results [the numbers in parentheses are statistical errors on the last digit(s) shown]. A and B refer to the type of atom in the compound $A^{III}B^{V}$.

		Surface peak intensity (atoms/row)					
		A			B		
	Potential	Measured	Calculated	Difference	Measured	Calculated	Difference
GaP	IPM	3.97(7)	3.35(6)	0.62(9)	5.2(3)	4.69(6)	0.5(3)
	ZBL	4.28(7)	3.65(2)	0.63(7)	5.6(3)	4.60(4)	1.0(3)
	Molière	4.28(7)	3.51(5)	0.76(9)	5.6(3)	4.94(3)	0.7(3)
GaAs	IPM		4.10(2)	0.98(4)		4.20(2)	0.98(4)
	ZBL		4.20(5)	1.11(5)		4.32(3)	1.11(5)
	Molière		4.40(4)	1.11(5)		4.24(4)	1.11(5)
InP	IPM	4.89(7)	4.06(7)	0.83(10)	6.4(8)	6.66(8)	−0.2(8)
	ZBL	5.04(8)	4.02(3)	1.01(8)	6.6(8)	7.07(9)	−0.4(8)
	Molière	5.19(8)	4.07(6)	1.12(10)	6.8(8)	7.04(11)	−0.2(8)

simulation technique without any normalization procedure. As a consequence, the SP intensity for an ideal bulklike surface can be determined in the most reliable way. The uncertainty of the SP intensity of about few percent, due to the potential inaccuracy, was found. The method of analysis presented in this paper can also be applied to clean surfaces according to the chosen model of the surface. It seems that the present approach, providing improved accuracy of the analysis, could diminish some discrepancies which were found between results of the high-energy ion scattering and other surface-analysis methods.[33]

A weak, but clear, interdependence between the ion-atom potential, random stopping power, and thermal vibrational amplitudes has been established. The results of the present work are in reasonable agreement with the mean values of the previously published data. The present method is particularly valuable for the determination of thermal vibrational amplitudes. Often these data are either scarce or widely dispersed. Apart from their importance for analytical methods they can be used for testing different lattice-dynamics models, calculation of the Debye-Waller factors, etc.

It would be of great interest to extend the analysis to other axial, as well as planar, channels.

ACKNOWLEDGMENTS

The authors with to thank T. Czyżewski, J. Kaczanowski, S. Kwiatkowski, and R. Pietrak for their helpful assistance during the experiments.

[1]L. C. Feldman, J. W. Mayer, and S. T. Picraux, *Materials Analysis by Ion Channeling* (Academic, New York, 1982).
[2]H.-J. Grossmann and W. M. Gibson, Surf. Sci. **139**, 239 (1984).
[3]R. J. Smith, C. Hennessy, M. W. Kim, C. N. Whang, M. Worthington, and Xu Mingde, Phys. Rev. Lett. **58**, 702 (1987).
[4]J. H. Barrett, Phys. Rev. B **3**, 1527 (1971).
[5]I. Stensgaard, L. C. Feldman, and P. J. Silverman, Surf. Sci. **77**, 513 (1978).
[6]J. H. Barrett, Phys. Rev. B **20**, 3535 (1979).
[7]See, e.g., B. Schmeideskamp, P. Jonk, H. E. Roosendaal, and H. O. Lutz, Nucl. Instrum. Methods B **17**, 309 (1986), and references therein.
[8]Y. Peysson, B. Daudin, M. Dubus, and R. E. Benenson, Phys. Rev. B **34**, 8367 (1986).
[9]R. P. Sharma, L. E. Rehn, P. M. Baldo, and J. Z. Liu, Phys. Rev. B **38**, 9287 (1988).
[10]Supplied by Institute of Electronic Materials Technology, Warsaw, Poland.
[11]P. J. M. Smulders and D. O. Boerma, Nucl. Instrum. Methods B **29**, 471 (1987).
[12]A. Dygo and A. Turos, Nucl. Instrum. Methods B **18**, 115 (1987).
[13]J. F. Ziegler, J. P. Biersack, and U. Littmark, *The Stopping and Range of Ions in Solids* (Pergamon, New York, 1985), p. 41.
[14]G. Molière, Z. Naturforsch. **2a**, 133 (1947).
[15]F. J. Smith, Physica (Utrecht) **30**, 497 (1964).
[16]A. Dygo and A. Turos, Radiat. Eff. Lett. **85**, 237 (1985).
[17]T. G. Lewis and W. H. Payne, J. Assoc. Comp. Machinery **20**, 456 (1973).
[18]A. Dygo and A. Turos, Phys. Lett. A **127**, 281 (1988).
[19]J. F. Ziegler, *Helium Stopping Powers and Ranges in All Elemental Matter* (Pergamon, New York, 1977).
[20]E. Clementi and C. Roetti, At. Data Nucl. Data Tables **14**, 177 (1974).
[21]J. Lindhard, K. Dan Vidensk. Selsk., Mat.-Fys. Medd. **34**, No. 14 (1965).
[22]We mean simulations of backscattering spectra, as opposed to simulations of the nuclear encounter probability. To the best of our knowledge, there are only a few attempts to reproduce real experimental spectra by simulation; see Ref. 11 and R. Kaufmann, Kernforschungszentrum Karlsruhe Report No. KfK 2638, 1978 (unpublished).
[23]P. Sigmund and K. B. Winterbon, Nucl. Instrum. Methods **119**, 541 (1974).
[24]M. Blackman, in *Handbuch der Physik,* edited by S. Flügge (Springer, Berlin, 1955), Vol. VII, Pt. I, p. 325.
[25]B. W. Batterman and D. R. Chipman, Phys. Rev. **127**, 690 (1962).
[26]*International Tables for X-Ray Crystallography,* 2nd ed., edited by C. H. MacGillarry and G. D. Rieck (Kynoch, Birmingham, 1968), Vol. III, p. 232
[27]B. T. M. Willis and A. W. Pryor, *Thermal Vibrations in Crystallography* (Cambridge University Press, Cambridge, 1975).
[28]J. S. Reid, Acta Crystallogr. Sec. A **39**, 1 (1983).
[29]D. Pathinettam Padiyan, S. K. Mohanlal, and K. S. Chandrasekaran, Z. Phys. B **65**, 299 (1987).
[30]D. P. Jackson and J. H. Barrett, Comput. Phys. Commun. **13**, 157 (1977); Phys. Lett. **71A**, 359 (1979); J. H. Barrett and D. P. Jackson, Nucl. Instrum. Methods **170**, 115 (1980).
[31]R. Weil and W. O. Groves, J. Appl. Phys. **39**, 4049 (1968).
[32]L. C. Feldman, I. Stensgaard, P. J. Silverman, and T. E. Jackman, in *Proceedings of the International Conference on the Physics of SiO_2 and its Interfaces,* edited by S. T. Pantelides (Pergamon, Oxford, 1978), p. 344.
[33]C. B. Duke and A. Paton, Surf. Sci. **164**, L797 (1985).